eJSSNT Regular Paper

e-Journal of Surface Science and Nanotechnology **21**, XX−XX (2023)

Processes of Current Transport in p-Si-n-$(Si_2)_{1-y-z}(GaP)_y(ZnSe)_z$ Heterostructure Produced by Liquid Phase Epitaxy

A. S. Saidov,[a, †] A. Yu. Leyderman,[a] Sh. N. Usmonov,[a] U. Kh. Rakhmonov,[a] D. V. Saparov,[a] Q. T. Suyarov,[b] A. M. Akhmedov [c]

[a] *Physical-Technical Institute, Uzbekistan Academy of Sciences, Chingiz Aytmatov str 2B, Tashkent, 100084, Uzbekistan*
[b] *Chirchik State Pedagogical Institute, Chirchik, 111700 Uzbekistan*
[c] *Tashkent Institute of Irrigation and Agriculture Mechanization Engineers, Kory Niyoziy str. 39, 100000 Tashkent, Uzbekistan*
[†] *Corresponding author: amin@uzsci.net*

Received: 19 August, 2022; Accepted: 20 October, 2022; J-STAGE Advance Publication: 3 December, 2022; Published: 3 December, 2022

The possibility of growing multicomponent epitaxial films of a semiconductor solid solution of molecular substitution $(Si_2)_{1-y-z}(GaP)_y(ZnSe)_z$ on Si and GaP substrates by liquid-phase epitaxy is shown. The distribution profiles of the atoms of the solid solution components Ga, P, Zn, Se, and Si over the thickness of the epitaxial film have been determined. The current-voltage (I–V) characteristics of p-Si-n-$(Si_2)_{1-y-z}(GaP)_y(ZnSe)_z$ heterostructures have been studied. A temperature-independent I–V characteristic has been found, the existence of which is explained on the basis of a theory considering the possibility of "blurring" of the impurity level. By comparing the theoretical and experimental results, the half-width of the blurring band for the energy levels of atoms of Si_2 and GaP molecules was determined, which had values equal to 0.146 and 0.34 eV, respectively.

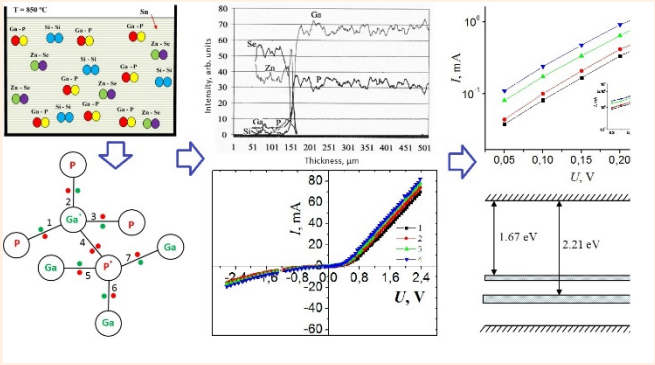

Keywords *Solid solution; Molecular substitution; Current-voltage characteristic; Injection depletion; Energy band*

I. INTRODUCTION

The synthesis of solid solutions based on several semiconductor materials makes it possible to control their fundamental properties such as a band gap, a spectral sensitivity region, etc., which are of great importance for the manufacture of modern optoelectronic devices [1−6]. In this regard, it is important to grow and study wide-gap semiconductor solid solutions with electrically passive isovalent impurities, the energy levels of which lie deep in the band gap of the base semiconductor. This will significantly expand the region of spectral sensitivity of a wide-gap material towards long waves and will make it possible to manufacture broadband photodetectors and photoconverters based on them [7−13]. This paper presents the results of a study on the growth of a $(Si_2)_{1-y-z}(GaP)_y(ZnSe)_z$ solid solution. The wide-gap semiconductor ZnSe (the band gap energy $E_{g,\,ZnSe}$ = 2.68 eV) was chosen as the base component, and isovalent GaP and Si_2 molecules were chosen as the impurity. Atoms of narrow-gap semiconductor molecules form deep energy levels located in the band gap of a wide-gap semiconductor [14]. The sums of the covalent radii of the atoms of the ZnSe, Si_2, and GaP molecules have close values with r_{ZnSe} = 2.45 Å, r_{Si2} = 2.34 Å, and r_{GaP} = 2.36 Å, and the sum of the valences of the atoms are equal among the ZnSe molecules ($Z_{Zn} + Z_{Se}$), Si_2 ($Z_{Si} + Z_{Si}$), and GaP ($Z_{Ga} + Z_P$). Mutual substitution of these molecules does not strongly deform the crystal lattice and does promote the formation of a solid solution of molecular substitution $(Si_2)_{1-x-y}(GaP)_x(ZnSe)_y$.

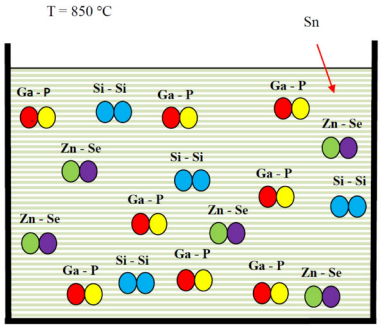

Figure 1: Dissolved GaP, ZnSe, and Si_2 molecules in Sn.

II. MATERIALS AND METHODS

For the formation of a substitutional solid solution between Si, GaP, and ZnSe, it is necessary to create conditions for molecular substitution. These conditions were created on the basis of a solution-melt model with molecular components [15] (Figure 1). According to this model, semiconductor compounds III-V and II-VI, when dissolved in metallic solvents at temperatures well below the melting point of these compounds, are mainly in the form of molecules. When GaP and ZnSe are dissolved in Sn at a temperature of 850°C, the GaP and ZnSe molecules do not decompose into individual Ga, P, Zn, and Se atoms but are in the form of the GaP and ZnSe molecules. The melting temperatures of GaP and ZnSe are 1477 and 1525°C, respectively, so that the temperature of 850°C is insufficient for complete breakage of Ga−P and Zn−Se bonds. The chemical bond between the atoms of compounds III-V and II-VI has both covalent and ionic characters. The crystal structure of GaP and ZnSe is cubic of the zinc blende type.

Let us consider the covalent-ionic nature of the GaP chemical bond. Figure 2 shows the covalent bonds of 8 atoms in the crystal lattice of the GaP binary compound. Each Ga atom forms a chemical bond with four P atoms; similarly, each P atom forms a chemical bond with four Ga atoms. The atoms located at the center of the corresponding tetrahedra are denoted as Ga* and P*. The Ga* atom has 3 valence electrons, and all of them will participate in the formation of covalent bonds with three neighboring P atoms [bonds (1), (2), and (3)]. The P* atom has 5 valence electrons, three of

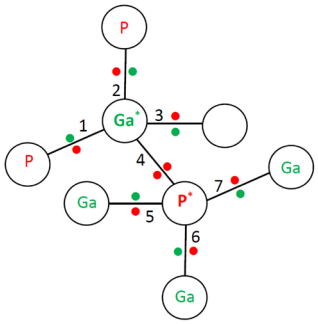

Figure 2: Covalent bonds of Ga and P atoms in the crystal lattice of GaP.

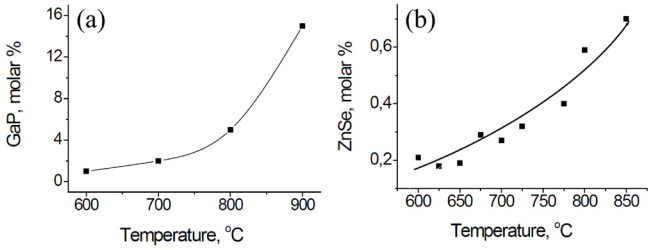

Figure 3: Temperature dependence of GaP (a) and ZnSe (b) solubility in Sn.

which participate in the formation of covalent bonds with three neighboring Ga atoms [bonds (5), (6), and (7)] (see Figure 2). The remaining two electrons participate in the formation of a chemical bond with the Ga* atom [bond (4)]. Since bonds (1), (2), (3), (5), (6), and (7) are formed due to the generalization of electrons of neighboring Ga and P atoms, and bond (4) is formed only due to two electrons of the P* atom and, then, apparently, the ionic fraction of chemical bond (4) will be stronger than the others. Therefore, bond (4) is stronger than the others. At certain temperatures, covalent bonds (1), (2), (3), (5), (6), and (7) (Figure 2) can break, while relatively strong bond (4) remains unchanged.

To prove the above model, experiments were carried out to study the solubility of GaP and ZnSe, as well as individual substances Ga, P, Zn and Se in Sn at 850°C.

As can be seen from the temperature dependence of the solubility of GaP and ZnSe in Sn, shown in Figure 3, with an increase in temperature from 600 to 850°C, the solubility of GaP increases from 1 to ~9.4 mol%, and ZnSe from 0.17 to 0.7 mol%. Separate substances Ga, P, Zn, and Se at 850°C are in a liquid or gaseous state. If these substances are

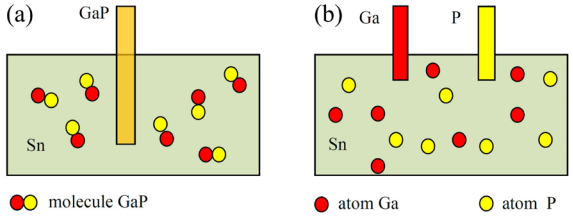

Figure 4: Dissolution of gallium phosphide in the form of GaP molecules (a) and of gallium and phosphorus in the form of individual Ga and P atoms (b) in Sn at a temperature of 850°C.

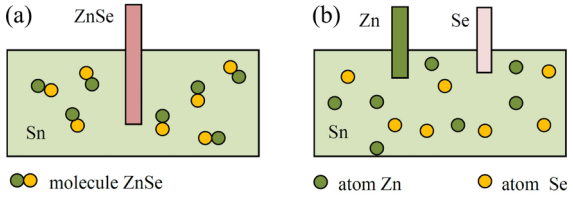

Figure 5: Dissolution of zinc selenide in the form of ZnSe molecules (a) and of zinc and selenium in the form of individual Zn and Se atoms (b) in Sn at a temperature of 850°C.

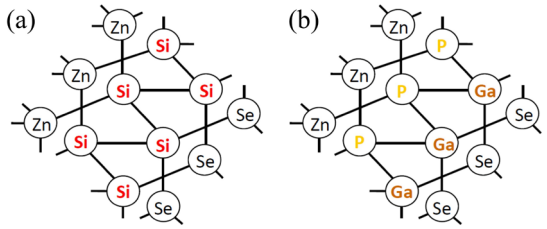

Figure 6: Spatial arrangement of atoms of the solid solution of molecular substitution $(Si_2)_{1-y-z}(GaP)_y(ZnSe)_z$, when a ZnSe molecule is replaced by two Si atoms (a) and a GaP molecule (b).

placed separately in liquid Sn, then Ga, P, Zn will completely dissolve at 850°C, and Se will dissolve within ~12 at% [Figures 4(b) and 5(b)]. Therefore, when dissolving GaP and ZnSe in Sn at 850°C, assuming that the GaP and ZnSe molecules are divided into individual Ga, P, Zn, and Se atoms, it can be assumed that the GaP or ZnSe crystal immersed in Sn should completely dissolve. This does not happen; the solubilities of GaP and ZnSe in Sn are limited. This indirectly confirms that GaP and ZnSe dissolved in Sn solution at temperatures up to 900°C are in the form of GaP and ZnSe molecules.

Since the binding energies of atoms of ZnSe, Si_2, and GaP molecules differ, the substitution of the ZnSe molecules by Si_2 or GaP molecules in the crystal lattice leads to a quantitative change in the forces of interaction between the nearest neighbors, but the covalent nature of the bond in the crystal lattice remains (Figure 6). As can be seen from Figure 6, when the ZnSe molecule is replaced by two Si atoms, the crystal lattice of the solid solution has covalent bonds such as Zn–Se, Zn–Si, Si–Si, and Si–Se, and there are covalent bonds of Ga–P, Ga–Se, Zn–Se, and Zn–P around the GaP molecules.

The chemical composition of the epitaxial layers of the $(Si_2)_{1-y-z}(GaP)_y(ZnSe)_z$ solid solution was examined by an X-ray microanalyzer (JSM 5910 LV, JEOL). The growth of solid solutions of molecular substitution $(Si_2)_{1-y-z}(GaP)_y(ZnSe)_z$ was carried out in a vertical-type quartz reactor (Figure 7).

The horizontally arranged substrates were fixed in a graphite cassette. The process of the growth of epitaxial films was carried out with forced cooling of a liquid Sn solution-melt in a hydrogen atmosphere. The solution-melt was poured into the space bounded by two substrates [16, 17]. Single-crystal wafers of p-type silicon and n-type gallium phosphide were used as substrates. The substrates had (111) crystallographic orientation, a thickness of 400 μm, and a diameter of 20 mm. The percentage ratio of the components of the solution-melt Sn-ZnSe-Si-GaP was calculated on the basis of preliminary results of the experimental studies and literature data [18–20]. When optimizing the film growth process, the following process parameters were varied: the initial crystallization temperature (T_s), the solution-melt cooling rate (υ), the solution-melt thickness (δ). The solid epitaxial films with mirror-smooth surfaces and good adhesion on the substrate surface were grown at T_s = 850°C, υ = 1°C min^{-1}, and δ = 1 mm. The epitaxial films had a thickness of ~30 μm and n-type conductivity.

III. RESULT AND DISCUSSION

Figure 8 shows the distribution profile of Si, Zn, Se, Ga, and P atoms of the epitaxial layer of the $(Si_2)_{1-y-z}(GaP)_y(ZnSe)_z$ solid solution grown on the GaP substrates. The analysis shows that the main component of the solid solution is the wide-gap ZnSe material.

When growing an epitaxial film on the GaP substrates, a layer of gallium phosphide grows from the very beginning. However, as the film grows, the molar content of Ga and P atoms rapidly decreases. These atoms are effectively replaced by silicon atoms. The substrate-film transition region is highly inhomogeneous. This area is enriched with silicon. The content of silicon atoms in the transition region first rapidly increases and then rapidly decreases. The content of

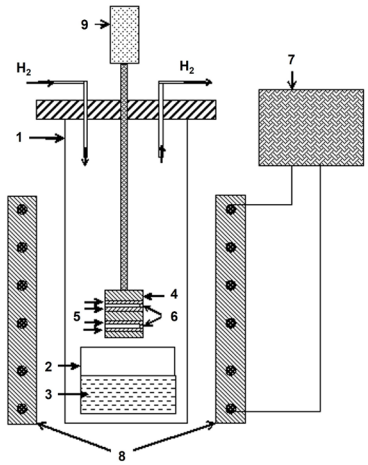

Figure 7: Drawing of a liquid-phase epitaxy installation: 1–a quartz reactor, 2–a quartz crucible, 3–solution-melt, 4–graphite cassette, 5–silicon substrates, 6–graphite supports, 7–control device, 8–heating blocks, and 9–an electric motor.

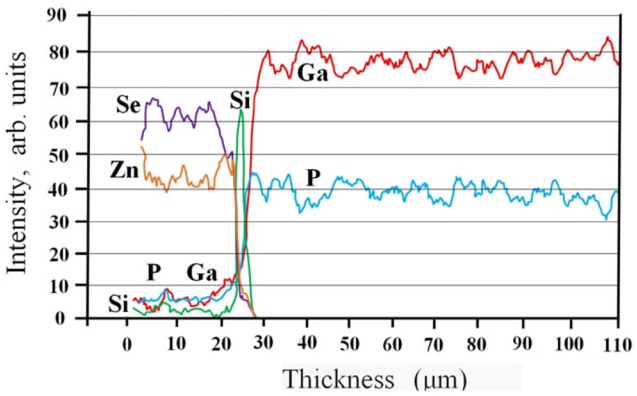

Figure 8: Distribution profile of Si, Zn, Se, Ga, and P atoms in the epitaxial layer of the $(Si_2)_{1-y-z}(GaP)_y(ZnSe)_z$ solid solution grown on the GaP substrates.

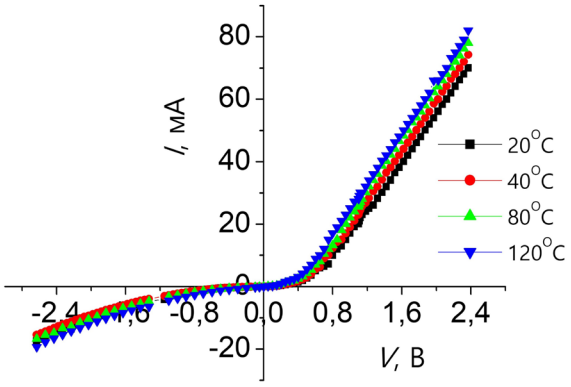

Figure 9: I–V characteristics of the p-Si-n-$(Si_2)_{1-y-z}(GaP)_y(ZnSe)_z$ heterostructure at different temperatures.

the Zn and Se atoms in the transition region increases monotonically from zero to ~40 at%. On the surface of the epitaxial film, the content of the Ga atoms was 3.7 at%, P 5.3 at%, Zn 46.8 at%, Se 43.2 at%, and Si 1 at%. In the near-surface region of the epitaxial film, a layer of a solid solution of molecular substitution $(Si_2)_{0.01}(GaP)_{0.09}(ZnSe)_{0.90}$ is formed.

To study the mechanisms of the current transfer in p-n structures, R_Ω–p-Si-n-$(Si_2)_{1-y-z}(GaP)_y(ZnSe)_z$–$R_\Omega$ structures were fabricated and their I–V characteristics were measured. R_Ω is current-collecting ohmic contacts. The Ohmic contacts were formed by vacuum deposition of silver-solid on the side of the substrate and quadrangular with an area of 12 mm^2 on the side of the epitaxial layer.

The I–V characteristics of the structures were recorded in the forward and reverse directions at various temperatures (Figure 9). Figure 9 shows that at all temperatures in the voltage range from 0 to 3 V, a current saturation is not observed. This suggests that the classical theory, which does not take into account the presence of impurities other than small doping donors and acceptors, is inapplicable here.

The I–V characteristics in the forward direction also does not correspond to the classical concepts. As can be seen from Figure 8 in the temperature range from 20 to 120°C, the I–V characteristic form does not practically change and its temperature dependence is very weak. Thus, we can say that, in this temperature range, we have a temperature-independent I–V characteristics. Traditionally, such I–V characteristics are usually explained by the tunneling mechanism of the passage of the current through the p-n junction. However, to implement this mechanism, it is necessary that the transition path should be narrow and the electric field should be strong. None of these conditions is satisfied for us, since our heterojunction was quite extended and the field was weak. There is another theory explaining the appearance of the I–V characteristics, which does not depend on the temperature. This theory is based on the effect of injection depletion, more precisely, the theory of the transformation of this effect under conditions of the existence of a blurred impurity spectrum in a semiconductor.

As is known, the electron and hole transport equations in the p-n structures are usually not considered separately, and the equation describing the so-called ambipolar transport of free carriers in the base of the p-n structure is obtained by mathematical transformations [21]:

$$D_a \frac{d^2p}{dx^2} - \vartheta_a \frac{dp}{dx} - U = 0,$$

where p is the concentration of charge carriers, x is the coordinate, ϑ_a is the ambipolar drift velocity of charge carriers, U is the recombination rate of nonequilibrium charge carriers, and D_a is the ambipolar diffusion coefficient of charge carriers, which is equal to

$$D_a = D_p \frac{2b(\gamma+1)}{b(\gamma+b+1)}.$$

The ambipolar drift velocity is generally determined by the expression:

$$\vartheta_a = \frac{\mu_a}{(b\gamma+b+1)p}\left\{N_d - \left[\frac{dE}{dx} - p\frac{\partial}{\partial p}\left(\frac{\partial E}{\partial x}\right)\right] + N_t^+ - p\frac{\partial}{\partial p}(N_t^+)\right\}E_J,$$

where $E_J = J/\left[q\mu_p(b\gamma+b+1)p\right]$ is the electric field in the base, $\gamma = N_t/p_{1t}$ is the sticking factor, N_t is the total concentration of trapping centers, N_t^+ is the number of trapping centers that captured hole, $p_{1t} = N_V \exp[-\Delta E_t/(kT)]$ is the Shockley-Read statistical factor for the level of trapping centers, $\Delta E_t = E_V - E_t$ is the activation energy of the level of trapping centers E_t, $\mu_a = \mu_n/(b\gamma+b+1)$ is the ambipolar mobility, $b = \mu_n/\mu_p$ is the ratio of the electron and hole mobilities, and J is the current density. It is known that terms proportional to dE/dx become significant in long p-n structures when $d/L \geq 10$, so they can be omitted in our case.

In our case of blurring of the impurity level, the ambipolar drift velocity takes the form [22]:

$$\vartheta_a = \frac{Jp^{-\alpha kT}}{qb\gamma}, \quad (1)$$

where $1/\alpha$ is the "characteristic" energy that determines the half-width of the blurring band of the impurity level. It follows from Eq. (1) that, in this case, the ambipolar drift velocity depends not only on the current density but also on the concentration of nonequilibrium carriers. Under these conditions, the injection characteristics are changed. In particular, instead of the well-known characteristic of the effect of injection depletion $V \sim \exp(aJd)$, we obtain the expression for the temperature-independent I–V characteristics in the form [22, 23]

$$J = J_0 e^{AqV}, \quad (2)$$

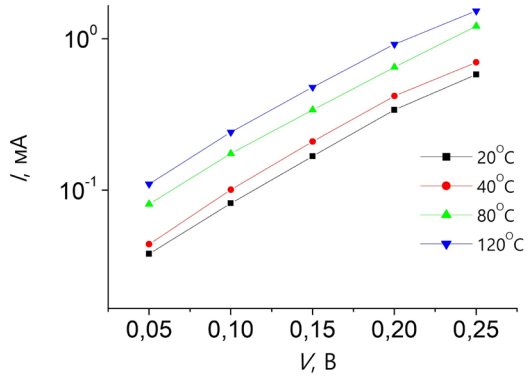

Figure 10: I–V characteristics of the p-Si-n-$(Si_2)_{1-y-z}(GaP)_y$-$(ZnSe)_z$ heterostructure on a semi-logarithmic scale in the voltage range from 0.05 to 0.25 V at different temperatures.

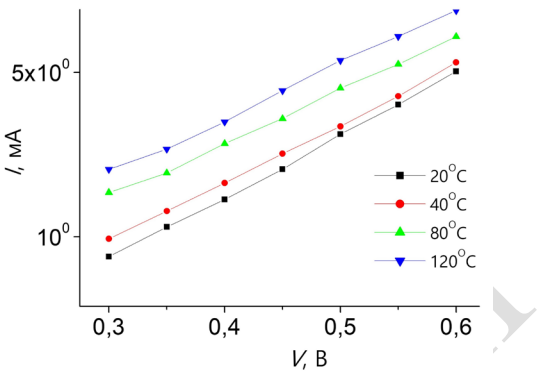

Figure 11: The same as Figure 10 but the voltage range from 0.3 to 0.6 V.

where $A = 2\alpha$. The parameter "A" can be calculated directly from the experiment using the formula: $A = \ln(J_2/J_1)/[q(V_2 - V_1)]$, q is the elementary charge. J_1 and J_2 are the current densities, and V_1 and V_2 are the voltages corresponding to two points of the exponential section of the I–V characteristic.

An analysis of the direct branch of the I–V characteristics of the structure shows that, in the initial section, the dependence $J = f(V)$ is practically independent of temperature and can be described by two successively replacing each other exponential dependences of the type Eq. (2) in the voltage range from 0.05 to 0.25 V and from 0.3 up to 0.6 V (Figure 9).

To determine the values of the parameter A, corresponding to two exponential sections of the I–V characteristics, we rebuilt these sections of the I–V characteristics on a semi-logarithmic scale (Figures 10 and 11). Analysis of the results shows that in the first section (at the voltages from 0.05 to 0.25 V), the parameter A takes the value $A_1 = 13.6$ eV^{-1} for all temperatures between 20 and 120°C. The half-width of the blurring band of the impurity level in this case is $1/\alpha = 0.146$ eV. In the second section of the I–V characteristics (at the voltages from 0.3 to 0.6 V) (Figure 11), the parameter A takes the value $A_2 = 5.79$ eV^{-1}, and the half-width of the blurring band of the impurity level is $1/\alpha = 0.34$ eV. The data obtained apparently indicate the formation of two deep blurred energy levels in the band gap of the solid solution $(Si_2)_{1-y-z}(GaP)_y(ZnSe)_z$.

With a further increase in the current, exponential dependences of the type Eq. (2) are replaced by power-law dependences of the type $J = BV^m$, with different values of the exponent m. In the area from 1.2 to 2.37 V, the m index decreases from 1.6 to 1.3 with an increase in the temperature from 30 to 120°C (Figure 9).

It should be emphasized that a number of conditions are necessary for the implementation of the effect of injection depletion, the main of which is the opposite direction of ambipolar diffusion and drift at the base of the p-n-n+ structure. At first glance, it seems that this is impossible in a p-n structure with an Ohmic rear contact. However, it should be remembered that we have a graded-gap semiconductor, the band gap in which varies greatly along the n-base (approximately from $E_{g,Si} = 1.1$ eV to $E_{g,ZnSe} = 2.7$ eV). In this case, any external influence (injection, temperature, etc.) will lead to the appearance of a concentration gradient $dp/dx > 0$, which is necessary to implement the effect of injection depletion. However, as the injection level increases, the contribution of the "quasi-electric" fields $E_{C(x)}$ and $E_{V(x)}$ becomes less and less significant, since they remain unchanged. This can lead to a violation of the equilibrium between ambipolar diffusion and drift and the appearance of a new power-law I–V characteristics pattern [22]:

$$J \approx V^{2/(1+\alpha kT)}.$$

Such an I–V characteristic qualitatively well explains the change in the exponent m from 1.6 to 1.3 in the experimental I–V characteristics curves in Figure 9. With increasing temperature, the exponent m in the dependence $J = BV^m$ decreases.

Previously, we studied the photoluminescence spectrum of an epitaxial layer of the $(ZnSe)_{0.88}(Si_2)_{0.03}(GaP)_{0.09}$ solid solution, grown on the GaP substrates from the liquid phase [24]. It is shown that, in addition to the main peak, the pho-

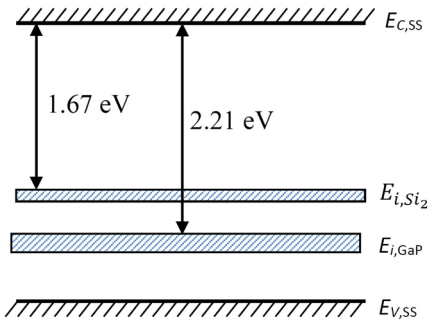

Figure 12: Energy band diagram of the $(ZnSe)_{0.90}(Si_2)_{0.01}(GaP)_{0.09}$ solid solution with a blurred band of energy levels $E_{i,Si2}$ and $E_{i,GaP}$ of the atoms of the Si_2 and GaP molecules, respectively. $E_{C,SS}$ is the bottom of the conduction band, and $E_{V,SS}$ is the top of the valence band of the solid solution.

toluminescence spectrum at a temperature of 5 K contains two more peaks at photon energies of 1.67 and 2.21 eV. These peaks are characterized by electronic transitions involving impurity energy levels of atoms of Si_2 and GaP molecules. The observed two exponential segments on the temperature-independent I–V characteristics apparently indicate that the atoms of the Si_2 and GaP molecules form a blurred band of deep energy levels located at $E_{i,\,Si2}$ = 1.67 eV and $E_{i,\,GaP}$ = 2.21 eV below the bottom of the conduction band of the solid solution, respectively. The half-width of the blurring band of the impurity level at $E_{i,\,Si2}$ = 1.67 eV is $\Delta E_{i,\,Si2}$ = 0.146 eV, and that at $E_{i,\,GaP}$ = 2.21 eV is $\Delta E_{i,\,GaP}$ = 0.34 eV (Figure 12).

IV. CONCLUSIONS

Liquid-phase epitaxy using metal solvents at temperatures well below the melting points of the solid solution components promotes the growth of semiconductor solid solution of molecular substitution. The possibility of obtaining a multicomponent solid solution of molecular substitution $(Si_2)_{1-y-z}(GaP)_y(ZnSe)_z$ with a blurred band of deep impurity energy levels of atoms of Si_2 and GaP molecules located in the band gap of the solid solution is shown. A wide-gap multicomponent semiconductor solid solution, the components of which form blurred bands of deep impurity energy levels, can be used to fabricate light-emitting diodes as well as to expand the spectral photosensitivity region of the base material in the long-wavelength region of the emission spectrum.

Acknowledgments

This work was financially supported by the Fundamental Research Programs of the Uzbekistan Academy of Sciences on the topic “Photovoltaic, thermal-voltaic, photothermal-voltaic and radiative effects in two and multicomponent semiconductor solid solutions with nanocrystals, obtained on silicon substrates from the liquid phase”.

References

[1] M. Lusi, Cryst. Growth Des. **18**, 3704 (2018).
[2] Yu. M. Andreev, V. V. Atuchin, G. V. Lanskii, N. V. Pervukhina, V. V. Popov, and N. C. Trocenco, Solid State Sci. **7**, 1188 (2005).
[3] A. Wu, J. Li, B. Liu, W. Yang, Y. Jiang, L. Liu, X. Zhang, C. Xiong, and X. Jiang, Dalton Trans. **46**, 2643 (2017).
[4] O. S. Vodoriz, T. V. Tavrina, G. O. Nikolaenko, and O. I. Rogachova, Metallofiz. Noveishie Tekhnol. **42**, 487 (2020) (in Ukrainian).
[5] B. Liu, J. Li, W. Yang, X. Zhang, X. Jiang, and Y. Bando, Small **13**, 1701998 (2017).
[6] M. Lusi, Cryst. Growth Des. **18**, 3704 (2018).
[7] Z.-H. Kang, J. Guo, Z.-S. Feng, J.-Y. Gao, J.-J. Xie, L.-M. Zhang, V. Atuchin, Y. Andreev, G. Lanskii, and A. Shaiduko, Appl. Phys. B **108**, 545 (2012).
[8] V. Garg, B. S. Sengar, G. Siddharth, S. Kumar, V. V. Atuchin, and S. Mukherjee, Surf. Interfaces **25**, 101146 (2021).
[9] X. Zhang, B. Liu, W. Yang, and X. Jiang, Prog. Nat. Sci. **26**, 312 (2016).
[10] Z. Ma, G. Li, X. Zhang, J. Li, C. Zhang, Y. Ma, J. Zhang, B. Leng, N. Usoltseva, V. An, and B. Liu, J. Mater. Sci. Technol. **85**, 255 (2021).
[11] J. Li, B. Liu, W. Yang, Y. Cho, X. Zhang, B. Dierre, T. Sekiguchi, A. Wu, and X. Jiang, Nanoscale **8**, 3694 (2016).
[12] R. Thomas, S. P. Thomas, H. Lakhotiya, A. H. Mamakhel, M. Bondesgaard, V. Birkedal, and B. B. Iversen, Chem. Sci. **12**, 12391 (2021).
[13] M. Fourmigué, J. Mater. Chem. C **9**, 10557 (2021).
[14] A. S. Saidov, Sh. N. Usmonov, D. V. Saparov, and A. M. Akhmedov, Appl. Sol. Energy **56**, 178 (2020).
[15] A. S. Saidov, Sh. N. Usmonov, and D. V. Saparov, Adv. Mater. Sci. Eng. **2019**, 3932195 (2019).
[16] A. S. Saidov, A. Sh. Razzakov, V. A. Risaeva, and E. A. Koschanov, Mater. Chem. Phys. **68**, 1 (2001).
[17] S. Nishida, K. Nakagawa, M. Iwane, Y. Iwasaki, N. Ukiyo, M. Mizutani, and T. Shoji, Sol. Energy Mater. Sol. Cells **65**, 525 (2001).
[18] A. S. Saidov, Sh. N. Usmonov, and D. V. Saparov, Adv. Mater. Sci. Eng. **2019**, 3932195 (2019).
[19] V. M. Andreev, L. M. Dolginov, and D. N. Tret'yakov, *Liquid Epitaxy in Technology of Semiconductor Devices* (Sov. Radio, Moscow, 1975) (in Russian).
[20] M. Hansen and K. Anderko, *Structures of Double Alloys*, Vol. I-II (Metallurgizdat, Moscow, 1962) (in Russian).
[21] E. I. Adirovich, P. M. Karageorgii-Alkalaev, A. Iu. Leiderman, *Double-Injection Currents in Semiconductors* (Izdatel'stvo Sovetskoe Radio, Moscow, 1978) (in Russian).
[22] P. M. Karageorgiy-Alkalaev and A. Yu. Leiderman, *Photosensitivity of Semiconductor Structures with Deep Impurities* (Fan, Tashkent, 1981) (in Russian).
[23] A. S. Achilov, Sh. A. Mirsagatov. Phys. Eng. Surf. **13**, 298 (2015) (in Russian).
[24] A. S. Saidov, S. N. Usmonov, U. K. Rakhmonov, A. N. Kurmantayev, and A. N. Bahtybayev, J. Mater. Sci. Res. **1**, 150 (2012).